

# Comparative assessment of entire bending-torsion fracture surface for 10HNAP steel using different optical measurement techniques

Dawid Zieliński<sup>1,2</sup>, Przemysław Podulka<sup>3</sup>, Cho-Pei Jiang<sup>4,5</sup>, Wojciech Macek<sup>1,2\*</sup> 

<sup>1</sup> Faculty of Mechanical Engineering and Ship Technology, Gdańsk University of Technology, ul. Gabriela Narutowicza 11/12, Gdańsk 80-233, Poland

<sup>2</sup> EkoTech Center, Gdańsk University of Technology, ul. Gabriela Narutowicza 11/12, Gdańsk 80-233, Poland

<sup>3</sup> Faculty of Mechanical Engineering and Aeronautics, Rzeszow University of Technology, aleja Powstanców Warszawy 12, 35-959 Rzeszów, Poland

<sup>4</sup> Department of Mechanical Engineering, National Taipei University of Technology, Taipei 10608, Taiwan

<sup>5</sup> High-Value Biomaterials Research and Commercialization Center, National Taipei University of Technology, Taipei 10608, Taiwan

\* Corresponding author's e-mail address: wojciech.macek@pg.edu.pl

## ABSTRACT

This research aimed to compare two microscopic measurement techniques – confocal and focus variation – for the assessment of the entire fracture surface method. The measurements were conducted using Sensofar S Neox 3D and Alicona InfiniteFocus G4 optical profilometers. Surface parameters were assessed for the entire fracture regions of the 10HNAP structural steel ring V-notched specimen. Fatigue test were performed under combination of bending and torsional moments. Stationary and ergodic random loadings had normal probability distribution and wide-band frequency spectra from 0 to 60 Hz. The obtained results for arithmetic mean height (Sa) and root mean square height (Sq) parameters did not show a comprehensible difference between the applied measurement techniques for the analysed specimen. Additionally, the process of filling in non-measured (NM) points does not significantly affect the results when compared to the raw data. Thus, both measurement devices and measurement techniques can be employed to the entire fracture method.

**Keywords:** steel, multiaxial fatigue, surface topography measurement techniques, entire fracture surface method.

## INTRODUCTION

Surface roughness is a fundamental output measurement of any manufacturing process [1, 2]. Topography and surface topology are especially important in such critical parts as turbine blades [3] or others [4]. The state of the surface structure greatly influences the structural and functional characteristics of the mechanical components [5,6]. Nonetheless, advanced surface topography parameters also indicate specific phenomena examined before [7], and after failure [8, 9]. Non-standard parameters that characterise complex surface topography are of particular interest, especially in the fracture surfaces of materials

experiencing multiaxial fatigue [10–12]. This is accomplished through increasingly sophisticated measurement systems and surface metrology software [13].

Measurement methods are generally categorised into mechanical and electromagnetic techniques, which can be further classified into contact and non-contact methods, facilitating measurements in both 2D and 3D systems [14]. Over the last years, a variety of instruments for measuring surface topography have been developed and made available for commercial use, owing to their effectiveness and versatility in assessing the form and texture of complex surfaces

[15]. There is an increasing demand for non-contact and online methods to measure these types of surfaces [16]. Currently, 3D optical profilometers are increasingly essential for achieving precise and consistent measurements across various techniques, including confocal [17], interferometric [18], and focus variation methods [19].

Over the previous 40 years, the procedures for quantifying and interpreting fracture surface topography grew continuously into an established technology that allows a fracture event to be reconstructed in microscopic detail. For instance, the authors of the paper [15] employed various optical devices and techniques, including confocal and focus variation methods, to assess the surface of the Ti6Al4V titanium alloy following finish turning under dry machining conditions. The results revealed a significant disparity in measurements between the devices, with differences of up to approximately 30%. The authors of a different study by Podulka et al. [20] evaluated the entire fracture surface method for the specimens made by explosive welding using a focus variation microscope and confocal measuring techniques. The appearance of mistakes in the form of noise and outliers was shown to cause differences in the measurement findings that were obtained. Additionally, the FRASTA method (fracture surface topography analysis) has been utilised to address a diverse range of failure issues [21, 22].

Taking into account the verification of the universality of the entire fracture surface method and other procedures for quantifying and interpreting fracture surface topography, it was decided to perform measurements in different ways. In this study, two different optical systems, i.e. Sensofar S Neox 3D and Alicona InfiniteFocus G4 optical profilometers were used to measure entire fracture surface topography for the fatigued 10HNAP structural steel ring V-notched specimen.

## MATERIALS AND METHODS

### Characteristics of test specimens

In the 1980s, Ahtelik, from Opole University of Technology, selected structural steel 10HNAP (S355J2G1W) as the test material [8]. 10HNAP is low-alloyed, higher-corrosion resistance steel, described by the Polish-European Standard (PN-EN 10155) [23]. Circumferential v-notched specimen (Fig. 1) was subjected to a bending-torsion fatigue test. A micro-computer, power amplifiers, electromagnetic inductors, and a random signal generator were all included in the fatigue machine. Random loadings had a normal probability distribution, were set to be stationary and ergodic, and had wide-band frequency spectra ranging from 0 to 60 Hz. A combination of torsional and bending moments with the same  $M_T$  and  $M_B$  values were generated during the fatigue test.

### Surface measurement devices

The fracture surface analysis was carried out using a 3D optical test stand, which allows data sets to be acquired at a high depth of focus. The Alicona InfiniteFocus G4 and Sensofar S Neox 3D instruments were used to measure the fracture surface topography. For the Alicona InfiniteFocus G4 profilometer, the magnification is 10x, while for the Sensofar S Neox 3D it is 5x. This difference is caused by the desire to verify measurement parameters while optimizing test time. The set of critical measurement conditions for the equipment used is shown in Table 1.

### Entire fracture surface method

The raw measurement data obtained were then analysed using specialised MountainsMAP premium 9.1 software as a post-processor. Source

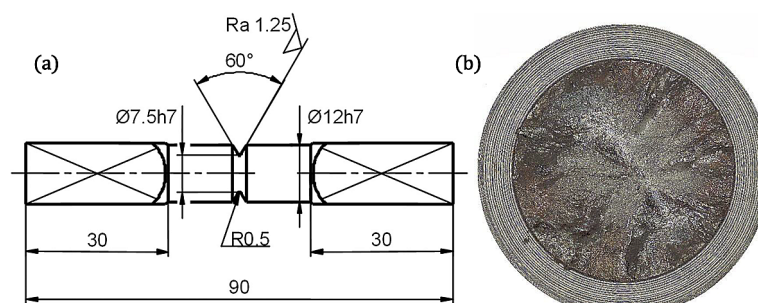


Figure 1. Tested specimen shape and dimensions (a); and fracture surface view (b)

**Table 1.** Set of the crucial measurement conditions for the devices used

Alicona G4 ×10 focus variation	Sensofar ×5 focus variation	Sensofar ×5 confocal
Model: IFM G4g Technique: FocusVariation Magnification: 9.99169x Soft version: IF-LaboratoryMeasurementModule 5.1 Number of Images: 11 rows x 9 columns Vertical Resolution: 360.7385nm Lateral Resolution: 3.9142µm Z scan: 1701 µm Exposure Time: 136.5 µs Contrast: 0.17 Elapsed Time: 1.781 h	Model: S neox 090 Technique: FocusVariation Magnification: 5.0000x Soft version: SensoSCAN S neox 7.7 Number of Images: 3 rows x 3 columns Topography: 3450 x 2882 px Area: 9.52 x 7.95 mm Pixel Size: 2.76 µm/pixel Z scan: 4602 µm Light: 8.32% Ring Light: 3.62% Threshold: 1.00% Measured: 85.73% Elapsed Time: 01:36 min	Model: S neox 090 Technique: Confocal Magnification: 5.0000x Soft version: SensoSCAN S neox 7.7 Number of Images: 3 rows x 3 columns Topography: 3445 x 2878 px Area: 9.51 x 7.94 mm Pixel Size: 2.76 µm/pixel Z scan: 4602 µm Light: 8.32% Ring Light: 3.62% Threshold: 1.00% Measured: 90.67% Elapsed Time: 02:16 min

files were transferred into the surface texture analysis software MountainsMap and resampled into height maps at a resolution automatically set by the software. The whole surface was reduced to eliminate the regions associated with the geometric discontinuities or missing points as well as to obtain uniform dimensions. An entire fracture

surface process was shown in Figure 2. The surface was limited to a circle with a diameter of 7.0 mm. The final measurement results were height parameters  $S_x$  according to ISO 25178 [24], fractal dimension (enclosing boxes method)  $D_f$  [25,26], texture isotropy [27] as well as a general view of the surface topography.

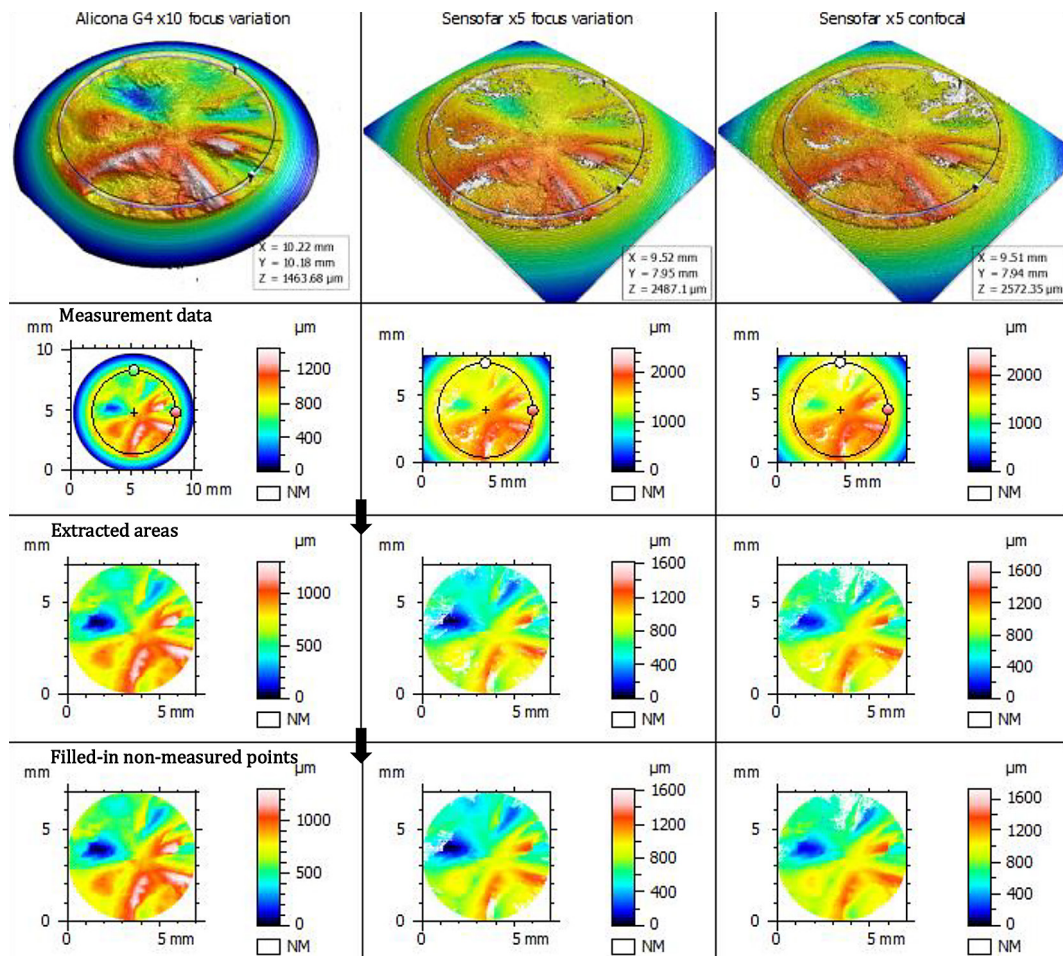


**Figure 2.** Scheme of the extracted area – region of interest (ROI) for a specimen subjected to bending-torsion loadings

## RESULTS AND DISCUSSION

The obtained  $S_x$  - height parameters measurement results for the both devices were included in Table 2 and 3 (before and after filling in missing data points [28]), while in Figure 3 the fractal dimension results were compared at different calculation resolutions [29, 30]. The texture isotropy is summarised in Figure 4. Finally, the comparison of all results was presented in Figure 5.

The differences in the results for the  $S_x$  - height parameters resulting from filling in the non-measured points (smooth shape from neighbors method) are insignificant. The surface topographies were also checked for resolution influence (Fig. 3). While partitioning of the surface, they have kept the track of number of iterations that take place. The resolution of the graph determines the number of iterations, and correspondingly, for ‘coarse resolutions’ it is 15 data points and for ‘Fine resolution’ it is 96 data points.

From Figure 3 it can be concluded that the focus variation technique (used on two different instruments) gives significantly lower values of the fractal dimension  $D_f$ . Filling the NMP has a negligible effect on the results of the fractal dimension  $D_f$ . Increasing the resolution of calculating the fractal dimension  $D_f$  affects the increase of its result. The fractal dimension  $D_f$  allows the use of fractional geometric dimensions, for instance for surfaces of dimension between 2 and 3. A surface having a fractal dimension of 2.08 (Sensofar  $\times 5$  focus variation. Coarse with non-measured

points) looks thus less complex than one having a dimension of 2.26 (Sensofar  $\times 5$  confocal fine with filled-in NMP); it is falsely said to be ‘nearer’ to a plane (2D) than to a volume (3D). The actual surface area is of course the same in both measurement cases.

The texture direction study, in MountainsMap premium 9.1 software, analyses the surface using the Fourier transform and shows dominant surface directions on a polar plot (see Fig. 4). It calculates the following parameters: (i) isotropy (the higher the percentage value the more the surface resembles itself in every direction); (ii) the three most dominant lay directions of a surface (in degree units). For all three cases, both Isotropy and the three most dominant lay directions assume similar values. The results presented in Table 2 and Figures 3–4 are summarised in Figure 5 in the form of bar graphs. Additionally, the elapsed time needed for individual measurements was presented, where: A(FV) – Alicona G4  $\times 10$  (focus variation technique); S(FV) – Sensofar  $\times 5$  (focus variation technique); S(CONF) – Sensofar  $\times 5$  (confocal technique).

## CONCLUSIONS

The most important conclusions and closing remarks are as follows. The differences in the results for the  $S_x$  - height parameters and custom parameters resulting from filling in the non-measured points (smooth shape from neighbors method) are insignificant:

**Table 2.** Set of measurement data before filling in missing data points for the analysed  $S_x$  - height parameters values

Parameter	Unit	Alicona G4 $\times 10$ focus variation	Sensofar $\times 5$ focus variation	Sensofar $\times 5$ confocal
Sq	$\mu\text{m}$	233.41	242.54	241.15
Sp	$\mu\text{m}$	612.04	912.76	917.25
Sv	$\mu\text{m}$	696.69	710.16	810.63
Sz	$\mu\text{m}$	1308.73	1622.92	1727.88
Sa	$\mu\text{m}$	190.63	200.86	198.43

**Table 3.** Set of measurement data after filling in missing data points for the analysed  $S_x$  - height parameters values

Parameter	Unit	Alicona G4 $\times 10$ focus variation	Sensofar $\times 5$ focus variation	Sensofar $\times 5$ confocal
Sq	$\mu\text{m}$	233.38	241.05	240.84
Sp	$\mu\text{m}$	612.06	912.11	917.08
Sv	$\mu\text{m}$	696.67	710.82	810.80
Sz	$\mu\text{m}$	1308.73	1622.92	1727.88
Sa	$\mu\text{m}$	190.60	199.59	198.16

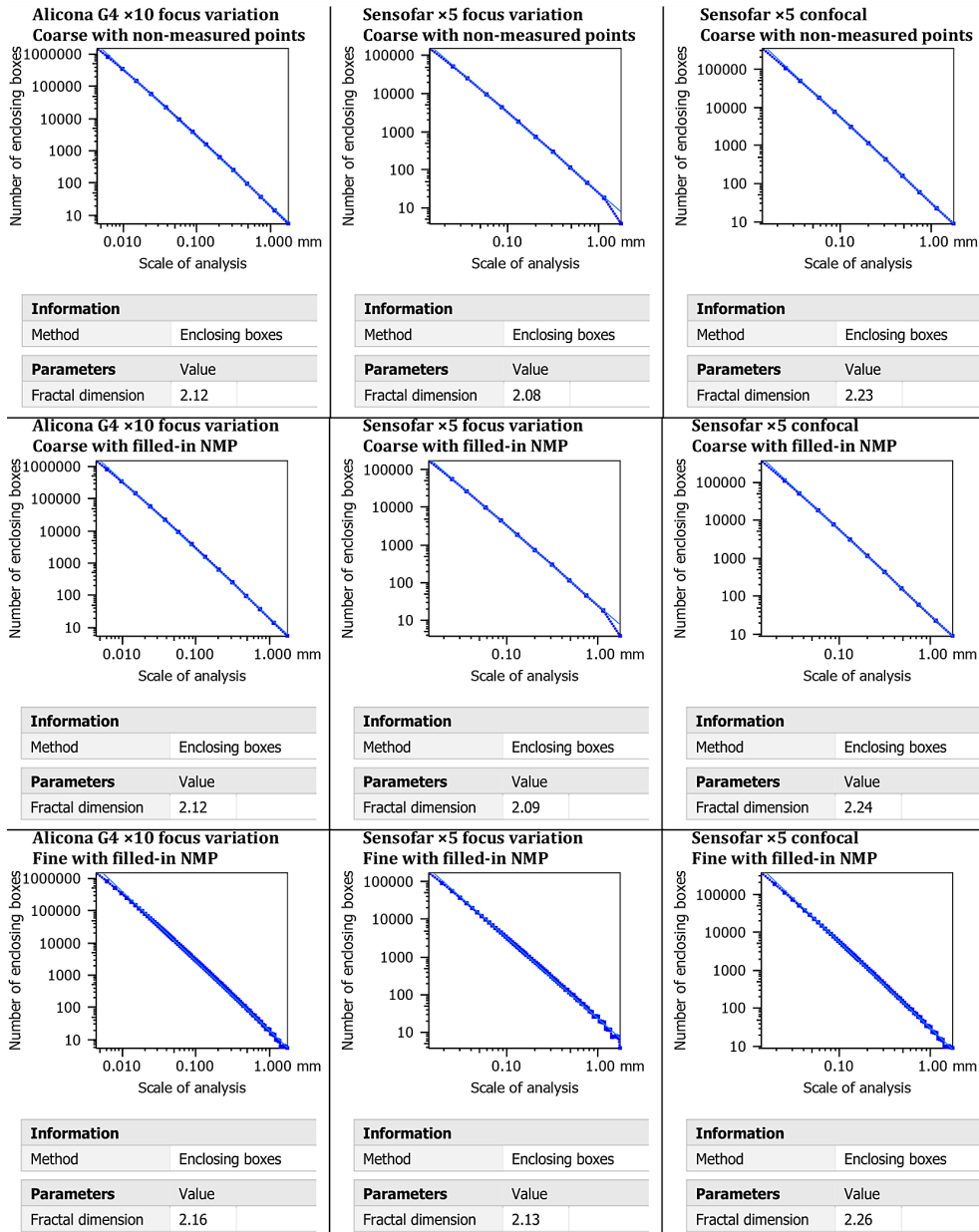


Figure 3. Fractal dimension  $D_f$  data obtained using individual parameters for the 10HNAP specimen after bending-torsion fatigue

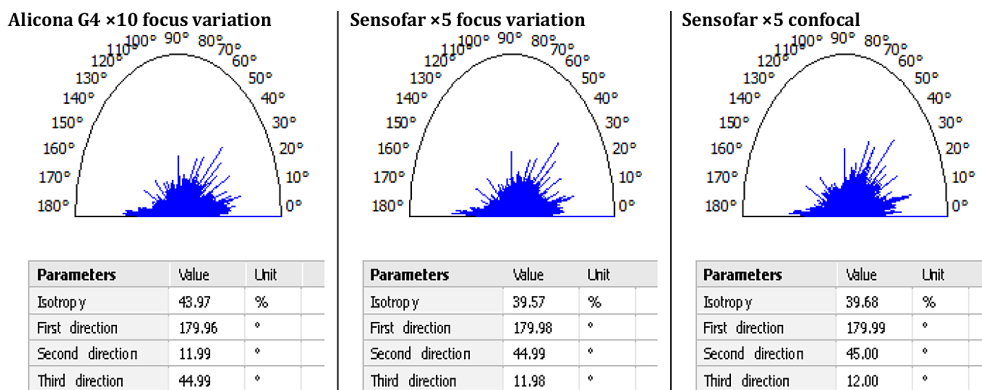


Figure 4. Texture direction analysis for the 10HNAP specimen after bending-torsion fatigue (with filled-in NMP)

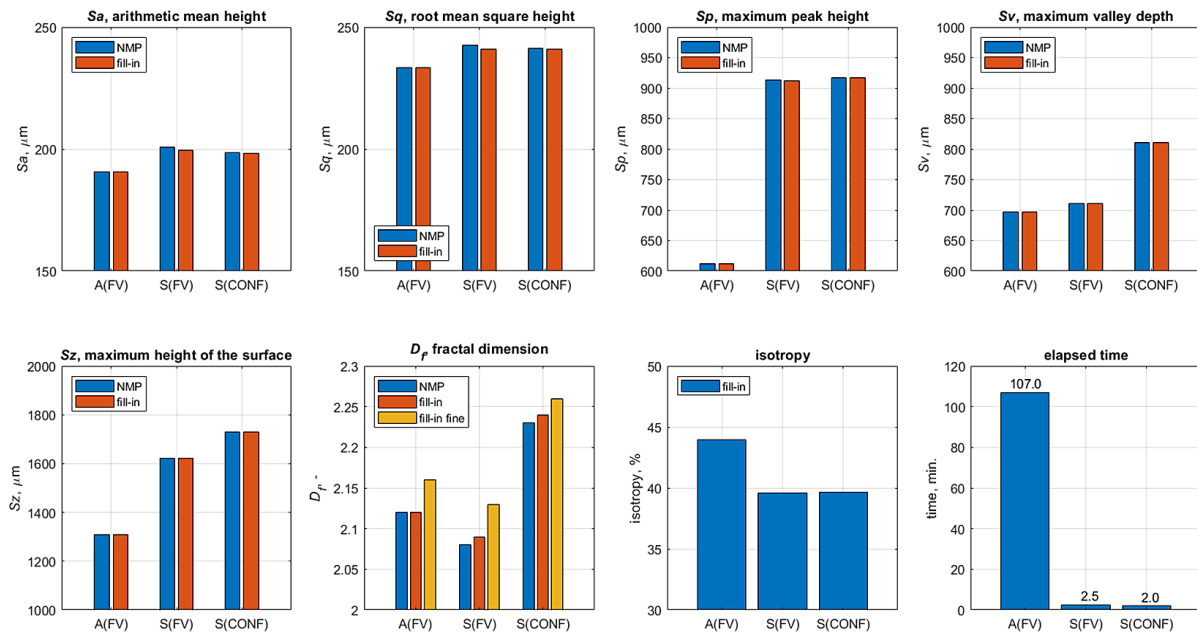


Figure 5. Bar graph for surface topography results grouped by data with NMP and fill-in for different measurement techniques

- for  $S_x$  group the largest difference was 0.64% for  $S_a$  parameter (Sensofar  $\times 5$  – focus variation technique);
- for fractal dimension  $D_f$  the largest difference was 0.48% also for Sensofar  $\times 5$  – focus variation technique case.

The focus variation technique (used on two different instruments) gives significantly lower values (5.2% and 7.2%) of the fractal dimension  $D_f$  than the confocal technique.

Increasing the resolution of calculating the fractal dimension  $D_f$  affects the increase of its result, and the largest increase occurred for Sensofar  $\times 5$  – focus variation technique, equal to 1.88%. Isotropy and the three most dominant lay directions assume similar values, regardless of the technique or instrument.

The Sensofar S Neox 3D optical profilometer enabled much faster measurements compared to the Alicona Infinite Focus G4 optical profilometer. The elapsed time for Sensofar was approximately 1.36 min for focus variation technique and 2.16 min for confocal technique, while the measurement on Alicona was longer at 786% and 495%, respectively. This could be important for measurements performed under industrial conditions in batch production of mechanical parts.

The measurement resolution on Alicona Infinite Focus G4 was higher, but this did not have

a significant impact on the results for the entire fracture surface method. Obtaining similar results of surface topography measurements for each of the presented devices and measurement techniques indicates a proper assessment of the surface structure with entire fracture surface method. Both measurement devices can therefore be used to measure the topography of this type of surface.

Another key point to note is that the entire fracture surface method holds significant promise for analysing failures in metals functioning under fatigue conditions. Furthermore, it may greatly assist in understanding the failure mechanisms resulting from various loads.

Future research directions include testing and detailed analysis of a wider range of materials, including advanced and hybrid materials. On the basis on the collected measurement data, it will be possible to further improve current measurement techniques and develop appropriate methods for their analysis.

### Acknowledgments

Financial support of these studies from Gdańsk University of Technology by the 2/1/2023/IDUB/13b/Ag grant under the Argentum Triggering Research Grants ‘Excellence Initiative – Research University’ program is gratefully acknowledged.

## REFERENCES

- Podulka P, Macek W, Szala M, Kubit A, Das KC, Królczyk G. Evaluation of high-frequency roughness measurement errors for composite and ceramic surfaces after machining. *J Manuf Process* 2024; 121: 150–71. <https://doi.org/10.1016/J.JMAPRO.2024.05.032>
- Krolczyk GM, Krolczyk JB, Maruda RW, Legutko S, Tomaszewski M. Metrological changes in surface morphology of high-strength steels in manufacturing processes. *Measurement (Lond)* 2016; 88: 176–85. <https://doi.org/10.1016/j.measurement.2016.03.055>
- Jiang CP, Masurotin, Wibisono AT, Macek W, Ramezani M. Enhancing Internal Cooling Channel Design in Inconel 718 Turbine Blades via Laser Powder Bed Fusion: A Comprehensive Review of Surface Topography Enhancements. *International Journal of Precision Engineering and Manufacturing* 2024 26(2): 487–511. <https://doi.org/10.1007/S12541-024-01177-3>
- Kowal M, Szala M. Diagnosis of the microstructural and mechanical properties of over century-old steel railway bridge components. *Eng Fail Anal* 2020; 110: 104447. <https://doi.org/10.1016/J.ENGFAILANAL.2020.104447>
- Deja M, Zieliński D, Agebo SW. Study on the wear characteristics of a 3D printed tool in flat lapping of Al<sub>2</sub>O<sub>3</sub> ceramic materials. *Wear* 2024; 556–557: 205515. <https://doi.org/10.1016/J.WEAR.2024.205515>
- Pawlus P, Reizer R, Grzegorz , Królczyk M, Munish, Gupta K. A State of the art on surface texture creation modelling methods in machining. *Archives of Computational Methods in Engineering* 2025; 1–27. <https://doi.org/10.1007/S11831-025-10229-4>
- Romanelli L, Santus C, Macoretta G, Barsanti M, Monelli BD, Senegaglia I, et al. A TCD-based statistical method to assess the impact of surface roughness and pores on the fatigue strength of LPBF Inconel 718 specimens. *Int J Fatigue* 2025; 194: 108821. <https://doi.org/10.1016/J.IJFATIGUE.2025.108821>
- Macek W. Post-failure fracture surface analysis of notched steel specimens after bending-torsion fatigue. *Eng Fail Anal* 2019; 105: 1154–71. <https://doi.org/10.1016/J.ENGFAILANAL.2019.07.056>
- Maleki E, Bagherifard S, Bandini M, Guagliano M. Surface post-treatments for metal additive manufacturing: Progress, challenges, and opportunities. *Addit Manuf* 2021; 37: 101619. <https://doi.org/10.1016/J.ADDMA.2020.101619>
- Macek W. Fractal analysis of the bending-torsion fatigue fracture of aluminium alloy. *Eng Fail Anal* 2019; 99: 97–107. <https://doi.org/10.1016/j.engfailanal.2019.02.007>
- Kotowski P. Fractal dimension of metallic fracture surface. *Int J Fract* 2006. <https://doi.org/10.1007/s10704-006-8264-x>
- Gryguć A, Behravesh SB, Shaha SK, Jahed H, Wells M, Williams B, et al. Multiaxial cyclic behaviour of extruded and forged AZ80 Mg alloy. *Int J Fatigue* 2019; 127: 324–37. <https://doi.org/10.1016/J.IJFATIGUE.2019.06.015>
- Senin N, Thompson A, Leach RK. Characterisation of the topography of metal additive surface features with different measurement technologies. *Meas Sci Technol* 2017. <https://doi.org/10.1088/1361-6501/aa7ce2>
- Whitehouse DJ. Surface metrology. *Meas Sci Technol* 1997; 8: 955. <https://doi.org/10.1088/0957-0233/8/9/002>
- Leksycki K, Królczyk JB. Comparative assessment of the surface topography for different optical profilometry techniques after dry turning of Ti6Al4V titanium alloy. *Measurement* 2021; 169: 108378. <https://doi.org/10.1016/J.MEASUREMENT.2020.108378>
- Macek W, Branco R, Costa JD, Pereira C. Strain sequence effect on fatigue life and fracture surface topography of 7075-T651 aluminium alloy. *Mechanics of Materials* 2021; 160: 103972. <https://doi.org/10.1016/j.mechmat.2021.103972>
- Kowalczyk J, Madej M, Piotrowska K, Radoń-Kobus K. The Impact of a Movement Type on Tribological Properties of AlTiN Coating Deposited on HS6-5-2C Steel. *Advances in Science and Technology Research Journal* 2024; 18: 305–16. <https://doi.org/10.12913/22998624/185164>
- Niemczewska-Wójcik M, Madej M, Kowalczyk J, Piotrowska K. A comparative study of the surface topography in dry and wet turning using the confocal and interferometric modes. *Measurement* 2022; 204: 112144. <https://doi.org/10.1016/J.MEASUREMENT.2022.112144>
- Ruzova TA, Haddadi B. Surface roughness and its measurement methods - analytical review. *Results in Surfaces and Interfaces* 2025; 100441. <https://doi.org/10.1016/J.RSURFI.2025.100441>
- Podulka P, Macek W, Rozumek D, Żak K, Branco R. Topography measurement methods evaluation for entire bending-fatigued fracture surfaces of specimens obtained by explosive welding. *Measurement* 2024; 224: 113853. <https://doi.org/10.1016/J.MEASUREMENT.2023.113853>
- Macek W, Sampath D, Pejkowski Ł, Żak K. A brief note on monotonic and fatigue fracture events investigation of thin-walled tubular austenitic steel specimens via fracture surface topography analysis (FRASTA). *Eng Fail Anal* 2022; 134: 106048. <https://doi.org/10.1016/J.ENGFAILANAL.2022.106048>
- Cao YG, Zhang SH, Tanaka K. Calculation method for maximum low-cycle fatigue loads using

- FRASTA reconstruction data. *Int J Fract* 2013. <https://doi.org/10.1007/s10704-013-9862-z>
23. Podulka P, Macek W, Zima B, Kopec M, Branco R, Achtelek H. Fracture surface topography measurements analysis of low-alloyed corrosion resistant steel after bending-torsion fatigue tests. *Precis Eng* 2024; 89: 296–316. <https://doi.org/10.1016/J.PRECISIONENG.2024.07.002>
24. International Organisation of Standardization. ISO 25178. Geometric Product Specifications (GPS) – Surface Texture: Areal 2010.
25. Macek W, Campagnolo A. Correlation between Fractal Dimension and Areal Surface Parameters for Fracture Analysis after Bending-Torsion Fatigue. *Metals* 2021; 11: 1790. <https://doi.org/10.3390/MET11111790>
26. Mandelbrot BB, Passoja DannE, Paullay AJ. Fractal character of fracture surfaces of metals. *Nature* 1984; 308: 721–2. <https://doi.org/10.1038/308721a0>
27. Macek W, Rozumek D, Królczyk GM. Surface topography analysis based on fatigue fractures obtained with bending of the 2017A-T4 alloy. *Measurement (Lond)* 2020; 152: 107347. <https://doi.org/10.1016/j.measurement.2019.107347>
28. Queffelec A. An important comparison of software for Scale Sensitive Fractal Analysis : are ancient and new results compatible? *Peer Community In Archaeology* 2023. <https://doi.org/10.24072/PCI.ARCHAEO.100024>
29. Macek W. The impact of surface slope and calculation resolution on the fractal dimension for fractures of steels after bending-torsion fatigue. *Surf Topogr* 2022; 10: 015030. <https://doi.org/10.1088/2051-672X/AC58AE>
30. Florindo JB, Bruno OM. Texture analysis by multi-resolution fractal descriptors. *Expert Syst Appl* 2013; 40: 4022–8. <https://doi.org/10.1016/J.ESWA.2013.01.007>